

# Role of Lamé $\lambda$ in Estimating Porosity and Saturation from Seismic Velocities

*J.G. Berryman, P.A. Berge and B.P. Bonner*

This article was submitted to  
Society of Exploration Geophysicists Annual Meeting  
Houston, TX  
October 31-November 5, 1999

*U.S. Department of Energy*

Lawrence  
Livermore  
National  
Laboratory

**March 12, 1999**

## DISCLAIMER

This document was prepared as an account of work sponsored by an agency of the United States Government. Neither the United States Government nor the University of California nor any of their employees, makes any warranty, express or implied, or assumes any legal liability or responsibility for the accuracy, completeness, or usefulness of any information, apparatus, product, or process disclosed, or represents that its use would not infringe privately owned rights. Reference herein to any specific commercial product, process, or service by trade name, trademark, manufacturer, or otherwise, does not necessarily constitute or imply its endorsement, recommendation, or favoring by the United States Government or the University of California. The views and opinions of authors expressed herein do not necessarily state or reflect those of the United States Government or the University of California, and shall not be used for advertising or product endorsement purposes.

This is a preprint of a paper intended for publication in a journal or proceedings. Since changes may be made before publication, this preprint is made available with the understanding that it will not be cited or reproduced without the permission of the author.

This report has been reproduced  
directly from the best available copy.

Available to DOE and DOE contractors from the  
Office of Scientific and Technical Information  
P.O. Box 62, Oak Ridge, TN 37831  
Prices available from (423) 576-8401  
<http://apollo.osti.gov/bridge/>

Available to the public from the  
National Technical Information Service  
U.S. Department of Commerce  
5285 Port Royal Rd.,  
Springfield, VA 22161  
<http://www.ntis.gov/>

OR

Lawrence Livermore National Laboratory  
Technical Information Department's Digital Library  
<http://www.llnl.gov/tid/Library.html>

Role of Lamé  $\lambda$  in Estimating Porosity and  
Saturation from Seismic Velocities

*James G. Berryman, Patricia A. Berge, and Brian P. Bonner*  
*Lawrence Livermore National Laboratory*  
*P. O. Box 808 L-200*  
*Livermore, CA 94551-9900*

Fluids often play a pivotal role in earth sciences problems. The most common tool used to analyze the fluid content in rocks and sediments is measurement of seismic (compressional and shear) wave velocities in the earth. Liquids reside underground by saturating – or only partially saturating – existing void space (porosity) in rock or soil. Two of the most important, and most difficult to measure, properties of subsurface rocks and fluids are porosity and saturation level. Here we show a new method of estimating both porosity and saturation level from seismic data, by displaying data on plots emphasizing the Lamé parameter  $\lambda$ , determined from measured velocities. A mathematical trick associated with one plotting method produces universal and easily interpretable behavior for sedimentary and igneous rocks, various unconsolidated materials, and man-made materials, in that virtually all the seismic data analyzed plot along straight lines. The slopes of these lines correlate well with porosity, while the locations of the data points along the lines provide estimates of fluid saturation.

**Fluids in the earth.** Resolution of various practical and scientific issues in the earth sciences depends on knowledge of fluid properties underground. In environmental cleanup applications, the contaminant to be removed from the earth is often a liquid such as gasoline or oil, or ground water contaminated with traces of harmful chemicals. In commercial oil and gas exploration, the fluids of interest are hydrocarbons in liquid or gaseous form. In analysis of the earth structure, partially melted rock is key to determining temperature and local changes of structure in the mantle. In all of these cases the most common tool used to analyze the fluid content is measurements of seismic (compressional and shear) wave velocities in the earth. The sources of these waves may be naturally occurring such as earthquakes, or man-made such as reflection seismic surveys at the surface of the earth or more direct measurements using logging tools in either shallow or deep boreholes.

Underground fluids occupy voids between and among the solid earth grains. When liquid or gas completely fills interconnecting voids, a well-known result due to Gassmann<sup>1</sup> predicts how the composite elastic constants that determine velocities should depend on the fluid and drained rock or soil elastic constants and densities. Gassmann's is a low frequency result and both laboratory and well-log measurements of wave velocities at sonic and ultrasonic frequencies have been observed to deviate markedly from Gassmann's predictions. This is especially so for partial saturation conditions (*i.e.*, when the fluid in each pore is a mixture of gas and liquid). In some cases these deviations can be attributed<sup>2,3</sup> to "patchy saturation," meaning that some void regions are fully saturated with liquid and others are filled with gas, so that Gassmann's formulas apply locally (but not globally) and must be averaged to obtain the overall seismic velocity of the system. In other cases, neither Gassmann's formulas nor the "patchy saturation" model seem to apply to seismic data. In these cases a variety of possible reasons for the observed velocity discrepancies have been put forward, including viscoelastic effects (velocity decrement due to frequency-dependent attenuation), fluid-enhanced softening of intragranular cementing materials, chemical changes in wet clays that alter mechanical properties, etc.

The objective of the present study has therefore been to find a method of using seismic data to estimate porosity and saturation, regardless of whether the rock or soil fits the Gassmann, the patchy saturation, or some other model. Seismic data provide two measured parameters,  $v_p$  and  $v_s$  (compressional and shear wave velocities, respectively). Simple algebraic expressions relate  $v_p$  and  $v_s$  to the Lamé parameters  $\lambda$  and  $\mu$  of elasticity theory, and the overall density  $\rho$ .

These relationships are well-known,<sup>4,5</sup> but the parameter  $\lambda$  is seldom used to analyze seismic data. Our first new way of displaying seismic data is to plot data points in the  $(\rho/\mu, \lambda/\mu)$ -plane — instead of (for example) the  $(v_p, v_s)$ -plane. The advantage of this plot is that, when either Gassmann’s equations or the “patchy saturation” model applies, most of the data will fall on one of two straight lines. Significant deviations from these two expected behaviors then provide a clear indication that the data violate some of the assumptions in Gassmann’s simple model, and furthermore provide clues to help determine which assumptions are being violated. Our second innovation in displaying seismic data is to plot the points in the  $(\rho/\lambda, \mu/\lambda)$ -plane. This second approach involves the use of an easily understood mathematical trick that leads naturally to universal and easily interpreted behavior; virtually all laboratory data on partial saturation we have analyzed so far plot with minimal scatter along straight lines in this plane. The length and slope of these lines have quantitative implications for measurements of both partial saturation and porosity. We have used sonic and ultrasonic laboratory data in this study, but the results provide very strong indications that equally useful relationships among seismic parameters, porosity, and saturation will be obtained from seismic data collected in the field.

**Basics of elastic wave propagation.** For isotropic elastic materials there are two bulk sound wave speeds,<sup>4,5</sup> compressional  $v_p = \sqrt{(\lambda + 2\mu)/\rho}$  and shear  $v_s = \sqrt{\mu/\rho}$ . Here the Lamé parameters  $\lambda$  and  $\mu$  are the constants that appear in Hooke’s law relating stress to strain in an isotropic material. The constant  $\mu$  gives the dependence of shear stress on shear strain in the same direction. The constant  $\lambda$  gives the dependence of compressional or tensional stress on extensional or dilatational strains in orthogonal directions. For a porous system with porosity  $\phi$  (void volume fraction) in the range  $0 < \phi < 1$ , the overall density of the rock or sediment is just the volume weighted density given by  $\rho = (1 - \phi)\rho_s + \phi[S\rho_l + (1 - S)\rho_g]$ , where  $\rho_s, \rho_l, \rho_g$  are the densities of the constituent solid, liquid and gas, respectively, and  $S$  is the liquid saturation<sup>6</sup> (fraction of void space in the range  $0 \leq S \leq 1$ ). When liquid and gas are distributed uniformly in all pores and cracks, Gassmann’s equations say that, for quasistatic isotropic elasticity and low frequency wave propagation, the shear modulus  $\mu$  will be mechanically independent of the properties of any fluids present in the pores, while the overall bulk modulus  $\lambda + \frac{2}{3}\mu$  of the rock or sediment including the fluid depends in a known way on porosity and elastic properties of the fluid and dry rock or sediment.<sup>1</sup> Thus, in the Gassmann model, the Lamé parameter  $\lambda$  is elastically *dependent* on fluid properties, while  $\mu$  is not. As noted previously, the density  $\rho$  also depends on saturation. At low liquid saturations, the fluid bulk modulus is dominated by the gas, and therefore the effect of the liquid on  $\lambda$  is negligible until full saturation is approached. This means that both seismic velocities  $v_p$  and  $v_s$  will decrease with increasing fluid saturation<sup>6–8</sup> due to the “density effect,” *i.e.*, the only quantity changing is the density which increases in the denominators of both  $v_p^2$  and  $v_s^2$ . As full saturation is approached, the shear velocity continues its downward trend, while the compressional velocity suddenly (over a narrow range of change of saturation) shoots up to its full saturation value. An example<sup>9,10</sup> of this behavior is shown in Figure 1a. This is the expected (ideal) behavior of porous rocks at low frequencies (sonic and below).

**First new method of data display.** In order to separate effects of liquids on  $\lambda$  from the well-understood effects of liquids on  $\rho$ , while taking advantage of the fluid-effect independence of  $\mu$ , we will combine the  $v_p$  and  $v_s$  data into a new type of plot. For porous materials that satisfy Gassmann’s conditions and low enough frequencies, we expect that, if we were instead

to plot seismic velocity data in a two-dimensional array with one axis being  $\rho/\mu = 1/v_s^2$  and the other being the ratio  $\lambda/\mu = (v_p/v_s)^2 - 2$ , then the result should be a straight (horizontal) line until  $S \simeq 1$  (around 95% or higher), where the data should quickly rise to a value determined by the velocities at full liquid saturation. This behavior is observed in Figure 1b. Note that, although this behavior is qualitatively similar to that of  $v_p$  in Figure 1a, we are now using only the seismic velocities themselves (no saturation data is required to generate this plot, although in this case saturation can be inferred from it at least qualitatively). What we observe here is traditional Gassmann-Domenico predictions for partial saturation.

If all the other assumptions of the Gassmann model are satisfied, but the liquid and gas are not distributed uniformly (so that different pores have different saturation levels), then we have the circumstances that may better fit the “patchy saturation” model.<sup>2,3</sup> In that case, the plot of  $\lambda/\mu$  vs.  $\rho/\mu$ , instead of data following a horizontal line with a jump up at the high saturation end (*e.g.*, Figure 1b), the ideal patchy saturation model (for completely segregated liquid and gas pockets) would predict that the data should lie on another straight line connecting to the two end points (dry and saturated) on this plot. These straight lines have been superimposed on the plots<sup>9–11</sup> for Figures 1b, 1d, and 1f. The anticipated behavior has been observed in other data (for other materials) not shown here, but two distinctly different types of behavior are observed in Figures 1d and 1f.

These apparent discrepancies from expected behavior are resolved by including another display for these three sandstones<sup>9–11</sup> in Figures 2a,c,e and corresponding plots for three limestones<sup>12,13</sup> in Figures 2b,d,f. Now the ratio  $\lambda/\mu$  is plotted versus *saturation* measured in the laboratory, and we observe in all these cases that the basic plot structure we had anticipated for Figures 1b, 1d, and 1f are in fact confirmed. What we learn from this observation is that the quantity  $\rho/\mu$ , which we wanted to use as a proxy for the saturation  $S$ , is not a very good proxy at high frequencies. We can safely attribute the discrepancies in Figures 1b,d,f to effects of high frequency dispersion as predicted by Biot’s theory.<sup>14–16</sup> Even the seemingly odd negative slope of the patchy saturation lines in Figure 1f can be understood as a predicted high frequency effect on the shear velocity.<sup>17</sup>

This first new plotting method is limited by the implicit assumptions that the shear modulus is independent of the presence of fluids and that frequency dispersion for shear velocity is negligible. The assumption that the materials’ shear properties are independent of the fluid is based on theoretical predictions about mechanical behavior only, and any chemical interactions between fluid and rock that might soften grain contacts could easily account for some of these discrepancies. Fluid-induced swelling of interstitial clays is another possible source of discrepancy as is fluid-induced pressure effects if the fluid is overpressured and therefore tending to severely weaken the rock. All of the chemical effects mentioned should become active with even very small amounts of fluid present, and should not have any significant frequency dependence. On the other hand, there are frequency dependent (dispersion) effects predicted by Biot’s theory<sup>14–16</sup> of acoustics in porous media (this theory generalizes Gassmann’s theory to higher frequencies and has been shown to be a very reliable predictor of behavior in simple porous media<sup>18</sup>) that can lead to complications difficult to resolve with the severely frequency-band limited data that are normally available.

Fortunately, Cadoret and colleagues<sup>12,13</sup> have in recent years performed a very extensive series of tests on limestones, including both ultrasonic and sonic experiments and with different means of achieving various levels of partial saturation. Figure 2b shows results obtained for an

Estailades limestone at 500 kHz. This material behaves very much like the sandstones we have already considered here, and appears to obey the Gassmann predictions very well all the way up to the ultrasonic frequency regime. There were several other limestones that were found to have similar if not quite such good behavior. On the other hand, there were two limestone samples (a granular Lavoux limestone and an Espeil limestone) that were found have very strong dispersion in the ultrasonic frequency band. These materials do not behave as expected when the data are plotted as in either Figure 1 or Figure 2. However, since extensional wave and shear wave data at 1 kHz were also collected for these same samples, we have computed the necessary quantities using standard formulas and plotted them for these two materials in Figures 2d and 2f. We see that even for these two badly behaved materials (in the ultrasonic band) the plots at lower frequency become easy to interpret again. These results provide a very strong indication that plots such as those in Figure 1 will be readily interpreted for all porous materials at seismic frequencies.

**Another new method of data display.** By making two seemingly small changes in the method of display, we now arrive at one of the main points of this paper. Since the expected behavior for Gassmann materials as observed in Figure 1b is a horizontal straight line for most values of saturation (*i.e.*,  $\lambda/\mu$  is expected to be almost constant until high saturation levels are reached), it is natural to consider dividing  $\rho/\mu$  by  $\lambda/\mu$ , and then plotting the points again in the  $(\rho/\lambda, \mu/\lambda)$ -plane. In the straight-line portion of the curve from Figure 1b, the only effect will be a change of scale, but large changes will result in the points representing full saturation or nearly full saturation. The results of this new plotting method are displayed in Figure 3. We observe that in all cases the result is apparently a straight line. This linear behavior is expected for a Gassmann material, since  $\lambda$  is just a scaling factor,  $\mu$  is unaffected by saturation, and  $\rho$  is linearly dependent on saturation. It would also be expected for a non-Gassmann material in which the effect of fluids on  $\lambda$  was negligible compared to the effect on  $\mu$ . It may also be expected for the case of patchy saturation if chemical interactions cause  $\mu$  to change with saturation, because then  $\mu$  for the porous medium would be some weighted average of  $\mu$  for the dry case and  $\mu$  for the fully saturated, chemically altered portions of the rock.

Figure 3a shows the same sandstone data as Figure 1. Similar data for five limestone samples<sup>12,13</sup> are plotted in Figure 3b. The straight line correlation of the data in this display is clearly confirmed by the limestone data. Numerous other examples of the correlation have been observed. No examples of appropriate data for partially saturated samples with major deviations from this behavior have been observed, although an extensive survey of available data sets has been performed for materials including limestones, sandstones, granites, unconsolidated sands, and some artificial materials such as ceramics and glass beads. This straight line correlation is a very robust feature of partial saturation data. The mathematical trick that brings about this behavior will be explained in simple terms below following a brief discussion of the usefulness of this display.

**Porosity correlation.** An additional feature of displays of the type presented in Figure 3 is that the slopes of the straight lines, at least for samples of similar material character, are inversely correlated with the porosity of the samples. This observation is highlighted in Figures 3c and 3d. In Figure 3c, a series of fused glass-bead samples<sup>19</sup> of uniform composition were produced, with lower porosities being achieved by varying temperatures and length of sintering times. The porosities are distributed almost perfectly in Figure 3c, with the lower porosity lines having higher slopes and higher porosity lines having lower slopes. The experimental error in

the stated porosity measurements  $\simeq \pm 0.6\%$ , so that the main discrepancy observed here with misalignment between the samples at  $\phi = 36.0\%$  and  $\phi = 36.5\%$  suggests that this display may provide a more sensitive means of determining the porosity. Figure 2d shows similar behavior for very low porosity granite<sup>20</sup> ( $\phi \simeq 1\%$ ); as the pressure is increased, the porosity in the material is steadily decreased mostly due to crack closure.

**Why the second display of data is always approximately linear.** We can understand both the linearity and the apparent dependence of the data correlation on porosity in the second plotting method by understanding some simple facts about such displays. Consider a random variable  $X$ . If we display data on a plot of either  $X$  vs.  $X$  or  $1/X$  vs.  $1/X$ , the result will always be a perfect straight line. In both cases the slope of the straight line is exactly unity and the intercept of the line is the origin of the plot (0, 0). Now, if we have another variable  $Y$  and plot  $Y/X$  vs.  $1/X$ , then we need to consider two pertinent cases: (1) If  $Y = \text{constant}$ , then the plot of  $Y/X$  vs.  $X$  will again be a straight line and the intercept will again be the origin, but the slope will be  $Y$ , rather than unity. (2) If  $Y \neq \text{constant}$  but is a variable with small overall variation (small dynamic range), then the plot of  $Y/X$  vs.  $1/X$  will not generally be exactly a straight line. The slope will be given approximately by the average value of  $Y$  and the intercept will be near the origin, but its precise value will depend on the correlation (if any) of  $Y$  and  $X$ . In our second method of plotting, the variable  $\lambda/\rho$  plays the role of  $X$  and the variable  $v_s^2 = \mu/\rho$  plays the role of  $Y$ . The plots are approximately linear because this method of display puts the most highly variable combination of constants  $\lambda/\rho$  in the role of  $X$ , and the least variable combination of constants  $v_s^2$  in the role of  $Y$ . Furthermore, the slope of the observed lines is therefore correlated inversely with the porosity  $\phi$  because the slope is approximately the average value of  $v_s^2$  which is well-known to decrease monotonically with increasing porosity.

**Conclusions.** The new plotting methods described in this paper are promising methods for estimating both porosity and saturation from seismic data for complicated earth materials, whether or not they fit Gassmann's model<sup>1</sup> or the patchy saturation model.<sup>2,3</sup> The high frequency data considered here are more likely to present wave attenuation and dispersion effects that normally complicate these analyses, but apparently do not seriously affect our interpretations when they are based on Lamé's constant  $\lambda$  as long as the data are taken in a range of frequencies that avoids the large dispersive effects. Porosity is correlated inversely with the slopes of the lines in Figure 3. The main conclusion associated with Figure 2 is that saturation is approximately a monotonic function of  $\lambda/\mu$ , and therefore also of  $\mu/\lambda$  as in Figure 3. So saturation can be estimated from knowledge of location along the lines of Figure 3 and relative changes of saturation can be determined with some high level of confidence.

## REFERENCES

1. Gassmann, F., Über die elastizität poröser medien. *Vierteljahrsschrift der Naturforschenden Gesellschaft in Zürich*, **96**, 1–23 (1951).
2. Endres, A. L., & Knight, R., The effect of microscopic fluid distribution on elastic wave velocities. *Log Anal.* **30**, 437–444 (1989).
3. Dvorkin, J. & Nur, A., Acoustic signatures of patchy saturation. *Int. J. Solids Struct.* **35**, 4803–4810 (1998).

4. Ewing, W. M., Jardetsky, W. S., & Press, F., *Elastic Waves in Layered Media*, McGraw-Hill, New York, 1957.
5. Aki, K., & Richards, P. G., *Quantitative Seismology: Theory and Methods*, Vols. I & II, W. H. Freeman and Company, New York, 1980.
6. Domenico, S. N., Effect of water saturation on seismic reflectivity of sand reservoirs encased in shale. *Geophysics* **39**, 759–769 (1974).
7. Wyllie, M. R. J., Gregory, A. R., & Gardner, L. W., Elastic wave velocities in heterogeneous and porous media. *Geophysics*, **21**, 41–70 (1956).
8. Wyllie, M. R. J., Gregory, A. R., & Gardner, G. H. F., An experimental investigation of factors affecting elastic wave velocities in porous media. *Geophysics* **23**, 459–493 (1958).
9. Murphy, William F., III, *Effects of Microstructure and Pore Fluids on the Acoustic Properties of Granular Sedimentary Materials*, Ph.D. Dissertation, Stanford University, 1982.
10. Murphy, William F., III, Acoustic measures of partial gas saturation in tight sandstones. *J. Geophys. Res.* **89**, 11549–11559 (1984).
11. Knight, R., & Nolen-Hoeksema, R., A laboratory study of the dependence of elastic wave velocities on pore scale fluid distribution. *Geophys. Res. Lett.* **17**, 1529–1532 (1990).
12. Cadoret, T., *Effet de la saturation eau/gaz sur les propriétés acoustiques des roches. Étude aux fréquences sonores et ultrasonores*. Ph.D. Dissertation, Université de Paris VII, Paris, France, 1993.
13. Cadoret, T., Marion, D., & Zinszner, B., Influence of frequency and fluid distribution on elastic wave velocities in partially saturated limestones: *J. Geophys. Res.* **100**, 9789–9803 (1995).
14. Biot, M. A., Theory of propagation of elastic waves in a fluid-saturated porous solid. I. Low-frequency range. *J. Acoust. Soc. Am.* **28**, 168–178 (1956).
15. Biot, M. A., Theory of propagation of elastic waves in a fluid-saturated porous solid. II. Higher frequency range. *J. Acoust. Soc. Am.* **28**, 179–1791 (1956).
16. Biot, M. A., Mechanics of deformation and acoustic propagation in porous media. *J. Appl. Phys.* **33**, 1482–1498 (1962).
17. Berryman, J. G., Elastic wave propagation in fluid-saturated porous media. *J. Acoust. Soc. Am.* **69**, 416–424 (1981).
18. Berryman, J. G., 1995, Mixture theories for rock properties: *Rock Physics and Phase Relations: A Handbook of Physics Constants*, American Geophysical Union, Washington, D.C., pp. 205–228.
19. Berge, P. A., Bonner, B. P., & Berryman, J. G., Ultrasonic velocity-porosity relationships for sandstone analogs made from fused glass beads. *Geophysics* **60**, 108–119 (1995).

20. Nur, A., & Simmons, G., The effect of saturation on velocity in low porosity rocks. *Earth and Planet. Sci. Lett.* **7**, 183–193 (1969).

unconsolidated sand reservoir. *Geophysics* **41**, 882–894 (1976).

**Acknowledgments.** We thank Bill Murphy and Rosemarie Knight for providing access to their unpublished data. We thank Norman H. Sleep for his insight clarifying the significance of our second method of plotting seismic data. Work performed under the auspices of the U. S. Department of Energy by the Lawrence Livermore National Laboratory under contract No. W-7405-ENG-48 and supported specifically by the Geosciences Research Program of the DOE Office of Energy Research within the Office of Basic Energy Sciences, Division of Engineering and Geosciences, and by the Environmental Management Science Program of the Office of Environmental Management and the Office of Energy Research.

Correspondence and requests for materials should be addressed to J.G.B. (e-mail: berryman1@llnl.gov).

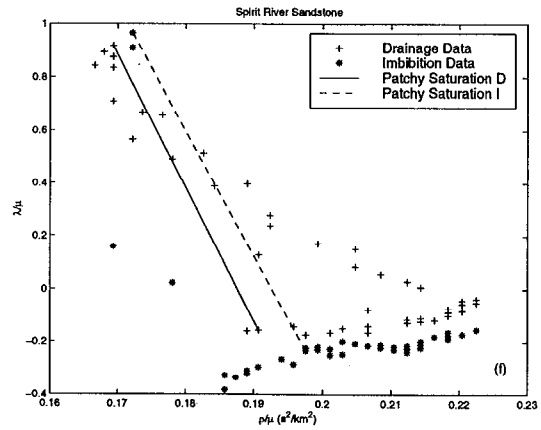
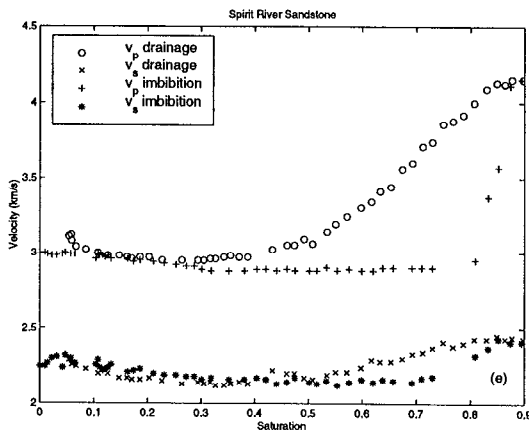
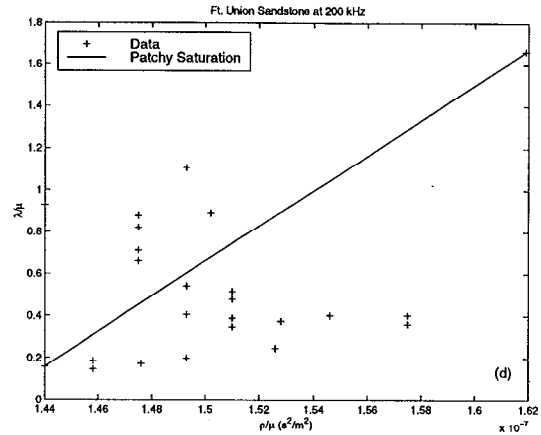
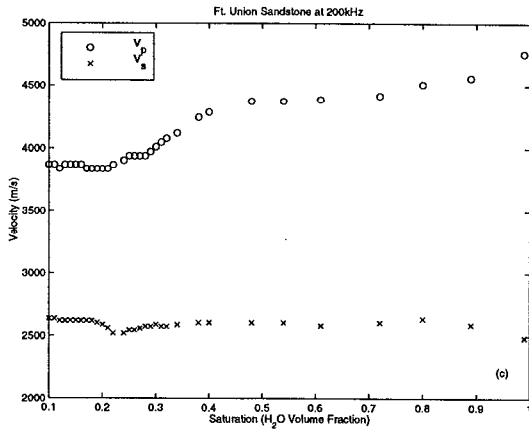
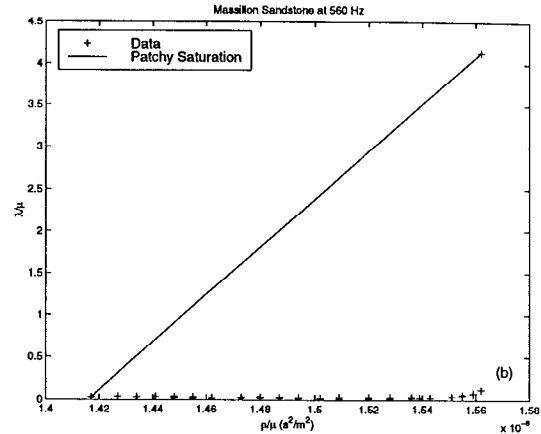
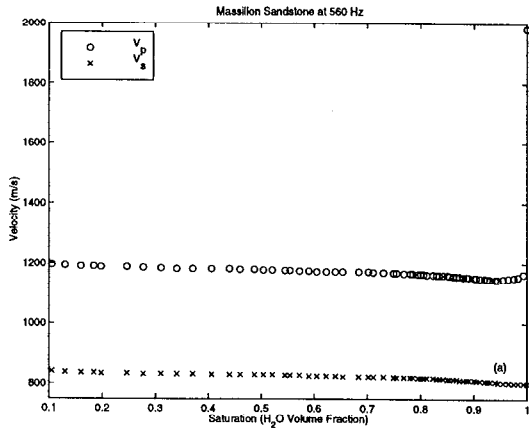
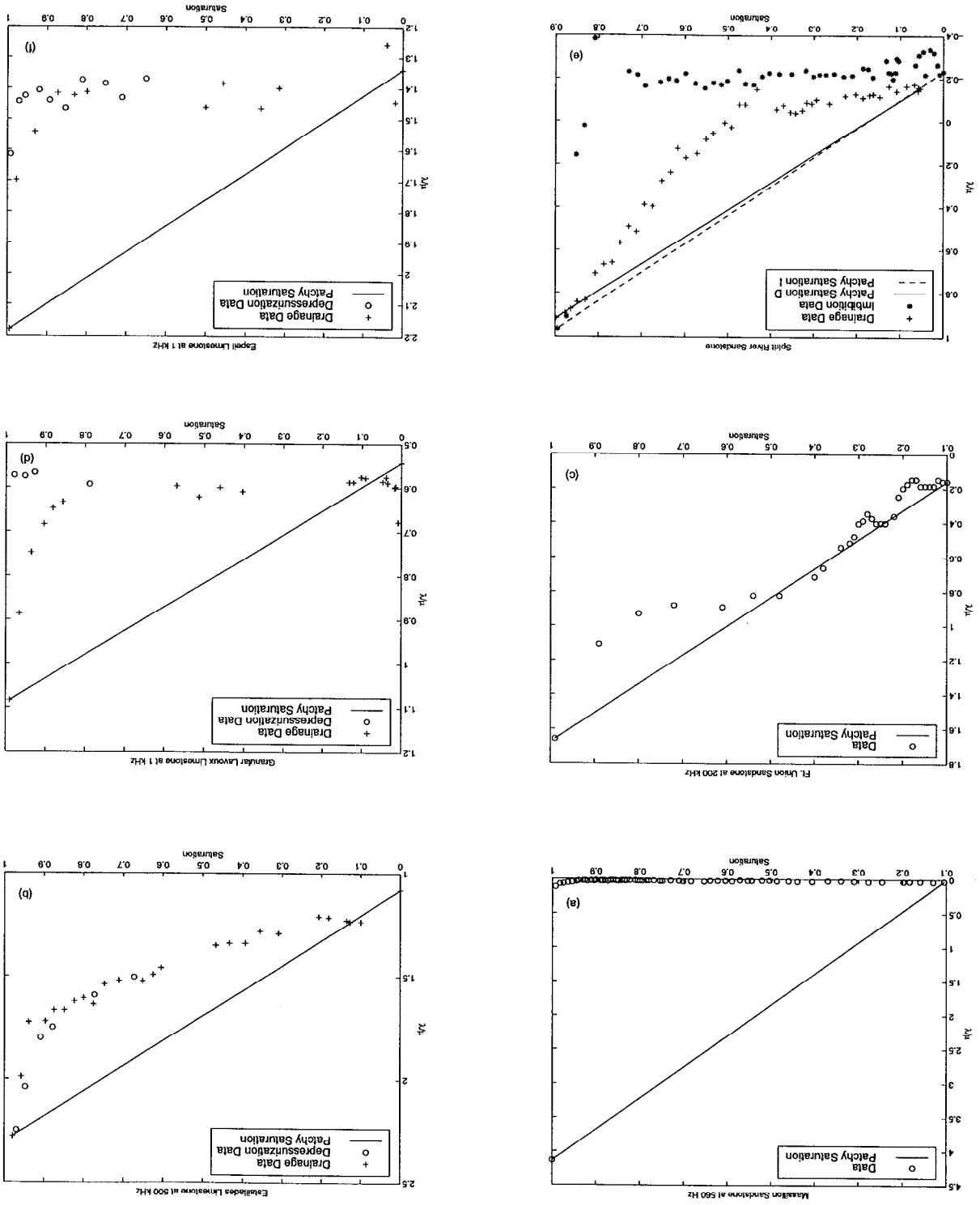


Figure 1: Compressional and shear velocities for Massillon and Ft. Union sandstone measured by Murphy<sup>9,10</sup> and for Spirit River sandstone measured by Knight and Nolen-Hoeksema.<sup>11</sup>

Figure 2: Ratio  $\lambda/\mu$  versus saturation for the three sandstones<sup>9-11</sup> of Figure 1 and for three limestones, 12,13



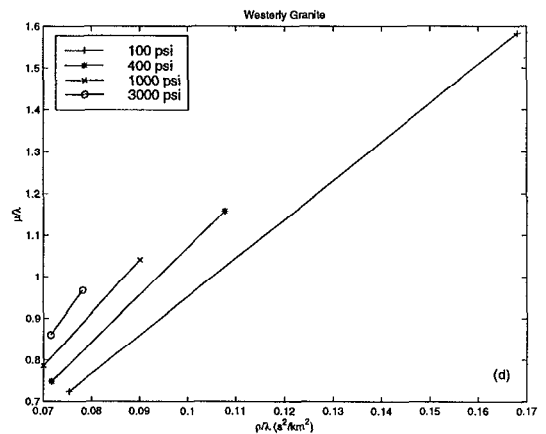
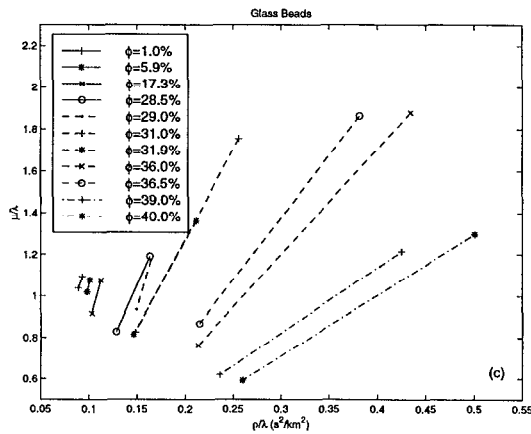
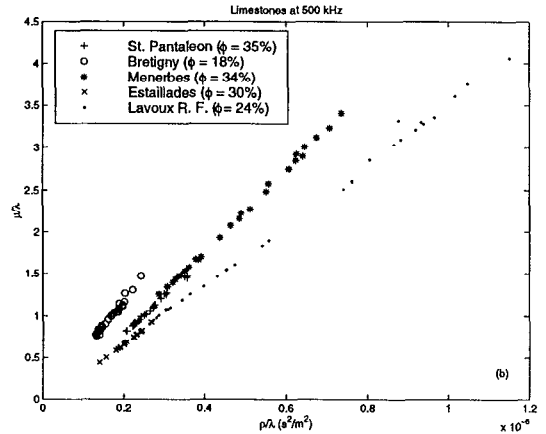
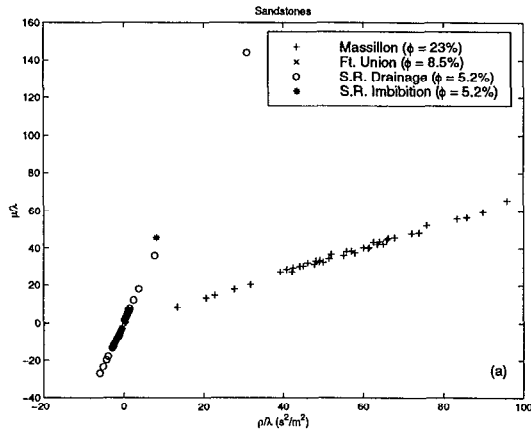


Figure 3: Examples of the correlation of slopes with porosity: (a) three sandstones,<sup>9-11</sup> (b) five limestones,<sup>12,13</sup> (c) 11 fused glass-bead samples,<sup>19</sup> (d) Westerly granite<sup>20</sup> at four pressures. The observed trend is that high porosity samples generally have lower slopes than lower porosities on these plots, although there are a few exceptions as discussed in the text. These trends are easily understood since the slopes are determined approximately by the average value of  $v_s^2$  for each material.